

Modelling the role of Atlantic air–sea interaction in the impact of Madden–Julian Oscillation on South American climate

Marcelo Barreiro¹  | Lina Sitz^{2,4,5} | Santiago de Mello¹ | Ramon Fuentes Franco³  |
Madeleine Renom¹ | Riccardo Farneti²

¹Departamento de Ciencias de la Atmósfera,
Facultad de Ciencias, Universidad de la Republica,
Montevideo, Uruguay

²Earth System Physics Section, The Abdus Salam
International Centre for Theoretical Physics,
Trieste, Italy

³Rosby Centre, Swedish Meteorological and
Hydrological Institute, Norrköping, Sweden

⁴Universidad Nacional del Sur, Bahia Blanca,
Argentina

⁵Instituto Nazionale di Oceanografia e di Geofisica
Sperimentale, Trieste, Italy

Correspondence

Marcelo Barreiro, Iguá 4225 esq. Matajojo,
Instituto de Física, Facultad de Ciencias,
Montevideo 11400, Uruguay.
Email: barreiro@fisica.edu.uy

This study addresses the role of Atlantic air–sea interaction in the remote influence of the Madden–Julian Oscillation (MJO) on eastern South American climate during austral summertime. To disentangle the different processes involved, reanalysis data as well as a regional climate model run in coupled mode and as a stand-alone atmosphere are used. The simulations are able to represent the observed influences of the MJO in precipitation and surface air temperature. In particular, in both setups the model is able to represent adequately the atmospheric teleconnections associated with the MJO, which involves the development of a barotropic cyclonic anomaly over South America between 30°S and 60°S, which favours a southwards shift of the South Atlantic Convergence Zone (SACZ) and a warming in eastern Brazil. Moreover, model simulations support the hypothesis that air–sea interaction is important to set up the strength of the rainfall response in the SACZ. That is, the development of a local warm SST anomaly forced by heat flux anomalies associated with the direct MJO impact in turn feeds back into the atmosphere generating a stronger surface convergence that shifts the SACZ southwards. In the absence of this SST-forced response the SACZ still shifts southwards, but anomalies are much weaker and less extensive. We also found that the coupled model represents more adequately the remotely forced MJO temperature signal over eastern Brazil, probably due to a too strong response of the stand-alone model to prescribed sea surface temperature.

KEYWORDS

air–sea interaction, MJO, regional climate model, South America, teleconnections

1 | INTRODUCTION

The Madden–Julian Oscillation (MJO) is the leading mode of variability on intra-seasonal timescales and it is known to affect remote regions through atmospheric teleconnections (e.g., Jones et al., 2004; Donald et al., 2006). The MJO's impact on South America and the physical mechanisms behind these atmospheric teleconnections have been studied by several authors (e.g., Paegle et al., 2000; Carvalho et al., 2004; de Souza and Ambrizzi, 2006; Gonzalez and Vera, 2014; Shimizu and Ambrizzi, 2015; Alvarez et al., 2016). In

particular, these studies show that during austral summertime the MJO affects climate over South America through two mechanisms: (a) a tropical–tropical connection that involves changes in the divergent circulation, (b) a tropical–extratropical connection that involves the forcing of extratropical Rossby waves from the Indo-Pacific towards the Atlantic basin.

These studies have emphasized the role of the atmospheric circulation anomalies induced by the MJO on the precipitation associated with the South Atlantic Convergence Zone (SACZ). The SACZ is a band of enhanced convection

that extends from the Amazon basin towards the South Atlantic and is an integral part of the South American monsoon (Vera et al., 2006). The variability of the SACZ affects a densely populated region and thus has been studied profusely. The SACZ shows variability not only on intra-seasonal, but also on synoptic, inter-annual and inter-decadal timescales (e.g., Carvalho et al., 2004). Previous studies have found that changes in the strength and position of the SACZ are strongly related to the path of extratropical atmospheric transients (Liebmann et al., 1999; Carvalho et al., 2004; Cunningham and Cavalcanti, 2006) and also to local sea surface temperature (SST) conditions. For example, atmospheric model simulations in Barreiro et al. (2002; 2005) have shown that on inter-annual timescales the SACZ shifts towards warm subtropical SST anomalies. Over land, however, the impact is small and in some cases the simulated response shows the opposite sign from the observed anomalies. Later, Chaves and Nobre (2004) showed that on seasonal timescales there is a negative feedback between the SACZ and the SST, so that an enhanced SACZ leads to a cooling of the SST below, through decreased solar insolation and enhanced latent heat fluxes, which then influences the atmosphere by damping the initial rainfall anomalies. Nobre et al. (2012) thus argue for a one-tier approach for seasonal climate prediction of rainfall in eastern Brazil.

Recently, Tirabassi et al. (2014) showed that the SACZ is one of the regions with the strongest two-way interaction between the ocean and the atmosphere. They found using a novel methodology that the air–sea coupling on synoptic timescales shows inter-annual variability. Most of the years there is no air–sea interaction or the atmosphere forces the ocean, but during some years the ocean forces rainfall variability in the SACZ and in some of those there is a two-way interaction. Furthermore, they found that the air–sea interaction that develops in the SACZ region depends on the trajectory of the atmospheric transients that lead to the original SACZ rainfall changes: the more oceanic the trajectory, the larger the impact of the ocean. They propose that the SST can modify the SACZ precipitation by enhancing the persistence of the anomalies providing a moisture source to sustain convection.

The above discussion suggests that Atlantic SST anomalies may play a role in the influence of the MJO on summertime climate over South America. However, this has not been addressed so far and has been neglected altogether. Here we analyse observations and reanalysis and perform numerical simulations with a regional coupled model to address this issue. In particular, we would like to answer the following questions: Is the MJO’s impact on South American climate independent of the regional SST? Moreover, Does the local Atlantic SST respond to MJO forcing and modulate its impact? We focus on eastern South America, which includes the SACZ region over Brazil, as well as the subtropics (Uruguay and northern Argentina).

We use (a) daily outgoing longwave radiation (OLR) from NOAA interpolated OLR data set (Liebmann and Smith, 1996) and (b) 10-m winds, 300-hPa meridional wind, surface air temperature, surface heat fluxes and SST from ERA-Interim (Dee et al., 2011) during the period January 1988 to December 1997. NOAA Interpolated OLR was downloaded from https://www.esrl.noaa.gov/psd/data/gridded/data.interp_OLR.html, ERA Interim data set was downloaded from <http://apps.ecmwf.int/datasets/data/interim-full-daily>.

All the analysis is performed using daily data for the summer season, which is considered to be from December to February (DJF). Thus, there are nine DJF seasons, each one spanning 90 days. Moreover, as we focus on intra-seasonal timescales, we calculate the daily anomalies by removing the daily annual cycle and also remove the inter-annual variability by removing the seasonal mean of each year.

2.1 | Model description and evaluation

The coupled model used is the RegCM-ES (Sitz et al., 2017) configured over the South Atlantic domain. The model is composed by the RegCM4.5 atmospheric model (Giorgi et al., 2012), extending from 55°S to 20°N and 145°W to 60°E and the MITgcm ocean model (Marshall et al., 1997), extending from 54°S to 10°N and from 70°W to 30°E). The region was designed to allow the representation of the path of atmospheric transients and teleconnection patterns associated with the main modes of rainfall variability in South America. Land processes are modelled with the Community Land Model 4.5 (CLM; Oleson et al., 2010). The model is configured to run with an atmospheric resolution of 50 km in the horizontal and 23 sigma/p vertical levels, while the ocean has a horizontal resolution of 1/8 of a degree and 40 vertical levels with finer resolution near the surface. Initial and lateral atmospheric boundary conditions are derived from ERA-Interim, whereas the ocean uses temperature, salinity and velocities from a global hindcast simulation using the ocean model MOM at 0.25° resolution. The atmosphere has prescribed historical SST as boundary condition in the regions outside the ocean model domain.

Two experiments are performed with the model during the period January 1988 to December 1997. In the first experiment the model is run fully coupled, while in a second experiment the atmospheric component of the model is forced with observed historical prescribed daily mean SSTs. The comparison between the two experiments allows to determine the role of ocean–atmosphere interaction in the basin. Hereafter we will call RegCM-ES when referring to the coupled run and RegCM when referring to the atmospheric-only experiment.

The mean summertime climatology of the model for both experiments is shown in Sitz et al. (2017). In the case of surface temperature, the RegCM-ES shows the typical

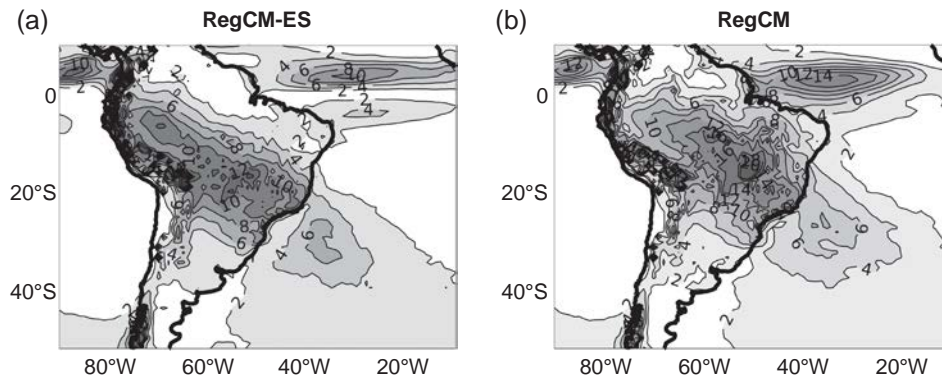


FIGURE 1 Climatology of DJF rainfall for (a) RegCM-ES and (b) RegCM. Contour interval is 2 mm/day

biases of coupled models in the Atlantic, that is a warm bias close to the western coast of Africa that extends towards the equator and a cold bias in the subtropical region off Brazil. Regarding precipitation, both models simulate the SACZ extending from the Amazon region towards the South Atlantic. Compared to the rainfall data set from the Global Precipitation Climatology Project (GPCP) (Huffman et al., 2001), RegCM-ES has a dry bias over South America to the north of 10°S and a wet bias between 10°S and 25°S, east of the Andes (Figure 1a). The stand alone RegCM has a strong wet bias over most of tropical South America except close to the equator (see Figure 1b).

To evaluate how the model performs on intra-seasonal timescales we calculated the leading Empirical Orthogonal Functions (EOFs) of rainfall after low-pass filtering the daily

mean data with a 10-day Lanczos filter (in addition to removing the seasonal cycle and inter-annual mean). The resulting data contain only intra-seasonal variability, that is, variability in the 10–90 days time range.

The two leading modes of intra-seasonal rainfall variability for the RegCM-ES and RegCM are shown in Figures 2 and 3, respectively. The corresponding modes for NOAA OLR are shown in Figure 4. Clearly, the leading EOF is the well-known dipole pattern that characterizes an intensified SACZ accompanied by less rainfall to the southwest over south Brazil (e.g., Nogues-Paegle and Mo, 1997). EOF1 explains 18% (20%) of the total variance in RegCM (RegCM-ES), similar to the one in NOAA OLR (24%). The principal components associated with the simulated EOF1 are correlated with that of NOAA OLR at 0.41 (0.31) for RegCM

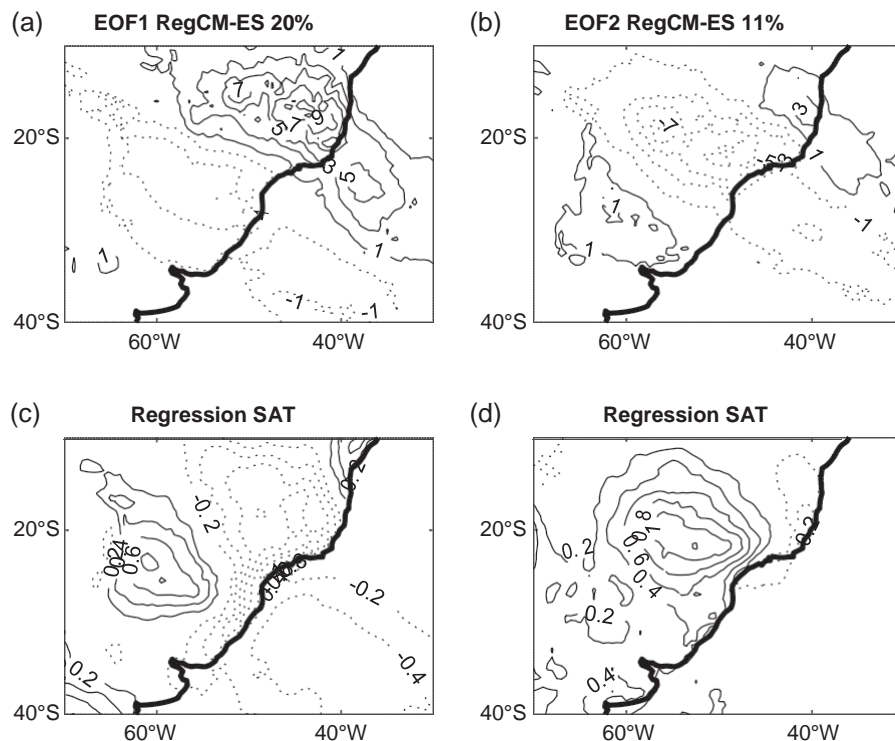


FIGURE 2 Leading modes of intra-seasonal rainfall variability in eastern South America during DJF for RegCM-ES. (a) Spatial pattern of EOF1 (mm/day), (c) linear regression of surface air temperature onto PC1 (K). Analogous variables for EOF2 are shown in (b, d)

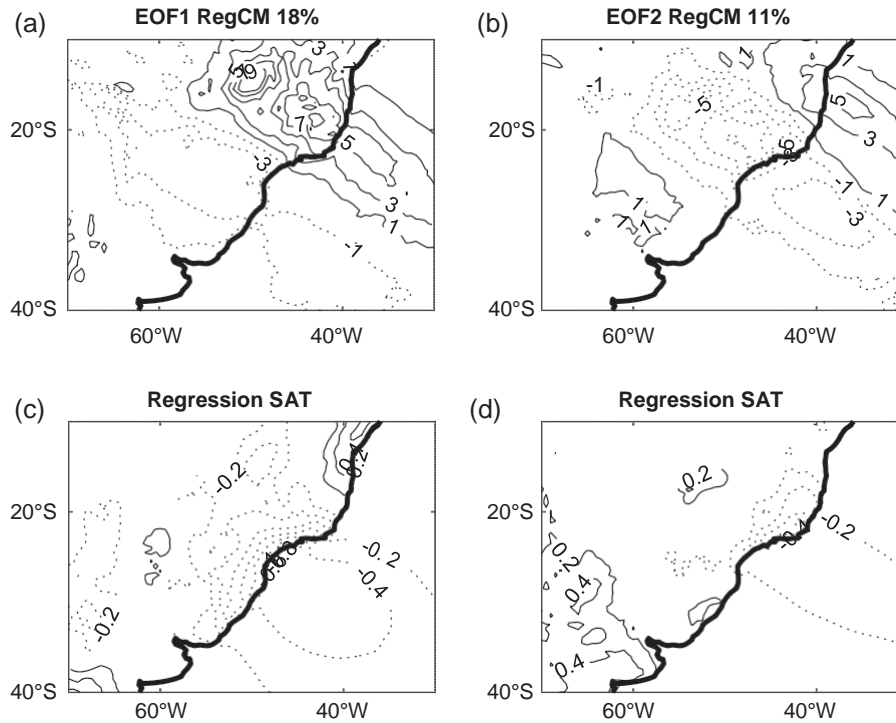


FIGURE 3 Same as Figure 2, but for RegCM

(RegCM-ES). Both correlations are statistically significant at 5% (taking into account the autocorrelation of the time series) suggesting that the boundary conditions (lateral and surface) partly control the evolution of the SACZ intra-seasonal variability. Moreover, if only days with magnitude of the principal component stronger than the standard deviation are considered, the correlation increases to 0.56 (0.42) for RegCM (RegCM-ES). The regression of surface air temperature shows a cooling in the inland region of stronger rainfall in eastern Brazil, seen in both models and reanalysis (cf., Figures 2–4). The negative correlation between rainfall and surface air temperature over land is expected because in tropical continents positive rainfall reduces insolation and also because the radiation is used for evaporation instead of for heating the surface (e.g., Trenberth and Shea, 2005; Barreiro and Diaz, 2011). Models, however, tend to have strongest cooling next to the coast, while reanalysis presents the largest cooling inland. Overall, the cooling pattern is better represented in RegCM-ES than in RegCM. On the other hand, RegCM-ES shows a strong warming in the region with decreased rainfall, which is not so pronounced in the reanalysis. Note that in the coastal region of Brazil and Uruguay south of 25°S there is cooling in a region of decreased rainfall that we will see in section 4 is associated with surface wind anomalies.

The second observed EOF (13%) shows a weakened SACZ flanked by two regions of enhanced convection to the northeast and west (Figure 4d). The simulations show a similar pattern and explain 11% of the total variance. The PC2 of RegCM-ES is correlated at 0.25 with the PC2 of NOAA OLR (significant at 5%), while the PC2 of RegCM is not significantly correlated. Notice that in RegCM the rainfall

anomalies that characterize EOF2 have a secondary maximum over the oceanic part of the SACZ, which is not present in RegCM-ES nor in the observations, suggesting that the RegCM responds too strongly to local SST anomalies, which is a common issue in AGCMs that sometimes leads to the wrong relationship between local SST anomalies and seasonal SACZ rainfall (Nobre et al., 2012). The surface air temperature shows positive anomalies in the region of decreased rainfall in both reanalysis and RegCM-ES.

2.2 | MJO characterization

In order to determine the MJO impact we use the RMM indices (Wheeler and Hendon, 2004) downloaded from the Data Library of the International Research Institute for Climate and Society (<https://iridl.ldeo.columbia.edu/SOURCES/.BoM/.MJO/.RMM/>). The propagating behaviour of the MJO is usually divided into eight different phases according to the values of the RMM1 and RMM2. In this study we grouped the eight phases into four groups according to the location of the MJO, that is we considered four states according to whether the MJO is located in the Western Hemisphere and Africa (phases 8 and 1, hereafter phase 18), Indian Ocean (phases 2 and 3, hereafter phase 23), Maritime Continent (phases 4 and 5, hereafter phase 45) and western Pacific (phases 6 and 7, hereafter phase 67). This allows to get more robust results given the shortness of the time period considered (nine summers). Also, atmospheric circulation anomalies are similar in consecutive phases (e.g., Alvarez et al., 2016). We considered MJO events as those that fulfil two conditions: (a) the amplitude is larger than 0.5 and (b) the

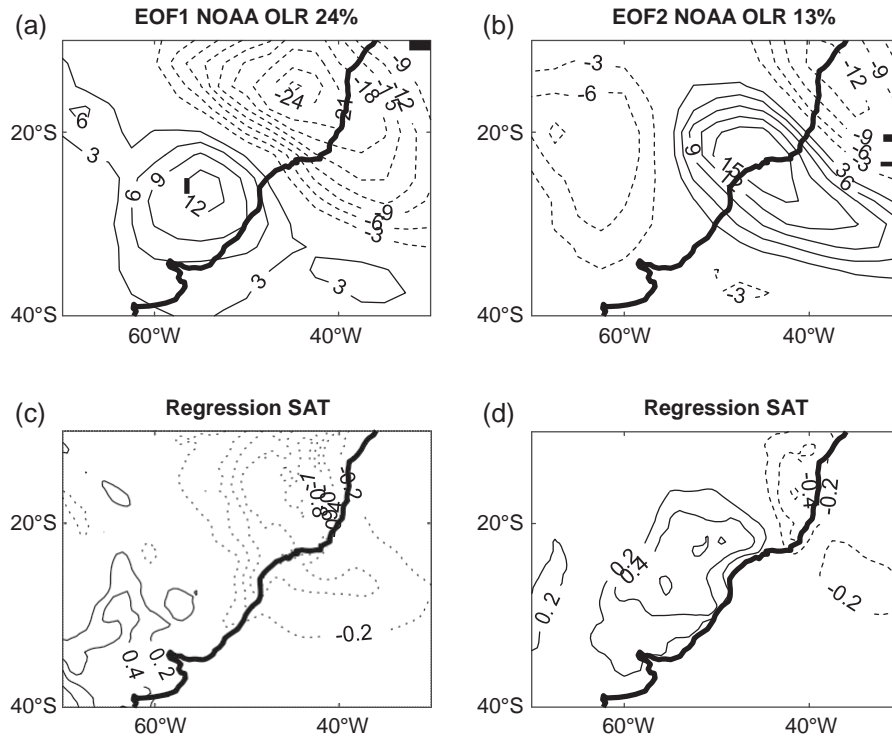


FIGURE 4 Same as Figure 2, but for NOAA OLR. In (a, b) units are W/m^2 and in (c, d) are K

MJO stays in one phase at least 5 days. This allows to filter out isolated days that have relatively large amplitude, and events will stay at least 10 days in one of the four phases. We have tested the results using different thresholds in amplitude and persistence and did not find a significant sensitivity. Moreover, imposing a filter that assures eastwards propagation as in Jones and Carvalho (2012) did not significantly affect the result. Thus, anomalies associated with the four different phases (18, 23, 45, 67) of a propagating MJO were calculated by constructing composites of the different observed and simulated fields according to the above criteria.

The statistical significance of the composites (positive–neutral) and (negative–neutral) was calculated using a difference of the mean t test, taking into account the serial autocorrelation of the time series to calculate the degrees of freedom. This is performed estimating the effective number of degrees of freedom $N_{eff} = N(1 - \rho)/(1 + \rho)$ (Wilks, 2011), where N is the number of days in each MJO phase and ρ is the lag1 autocorrelation of each (unfiltered) variable.

3 | RESULTS

3.1 | Rainfall and SST response

Figure 5 shows the OLR anomalies over South America associated with the different phases of the MJO. Phases 23 and 45 show a weaker than normal and southwards displaced SACZ, while phase 67 is characterized by a weakening of the continental Intertropical Convergence Zone

(ITCZ). The largest anomalies are found during phase 45 when the MJO is active over the Maritime continent and there is reduced convection over the Indian Ocean and the equatorial Pacific close to the dateline, in agreement with the literature (e.g., Alvarez et al., 2016). Previous authors have shown that during phases 8 and 1 (enhanced convection in Western Hemisphere and Africa) the SACZ strengthens (e.g., Shimizu and Ambrizzi, 2015; Alvarez et al., 2016), but even though there is a tendency in that direction our results do not show significant anomalies. This suggests that the MJO impact on eastern South American rainfall during these phases might not be as robust as during other phases, and may depend on the time period considered.

Accompanying these changes in precipitation, there are significant SST anomalies in the South Atlantic (Figure 5, right panels). In particular, phase 45 is characterized by a warm anomaly off eastern Brazil, below the SACZ. This warm anomaly persists until phase 67 and another small positive anomaly develops next to the coast between 20°S and 30°S, in the south Brazil bight. A cold anomaly also develops south of 40°S from phase 23 onwards that strengthens during phase 67.

By construction the composite of observed SST anomalies are a response to the atmospheric mechanical and thermodynamical forcing induced remotely by the MJO. However, once created they might influence the atmosphere above changing the evolution of circulation anomalies. In particular, it is interesting to note the development of the subtropical warm SST anomaly during phase 45 which is the one with largest SACZ response. This pattern of a weaker and southwards shifted SACZ together with a warm SST

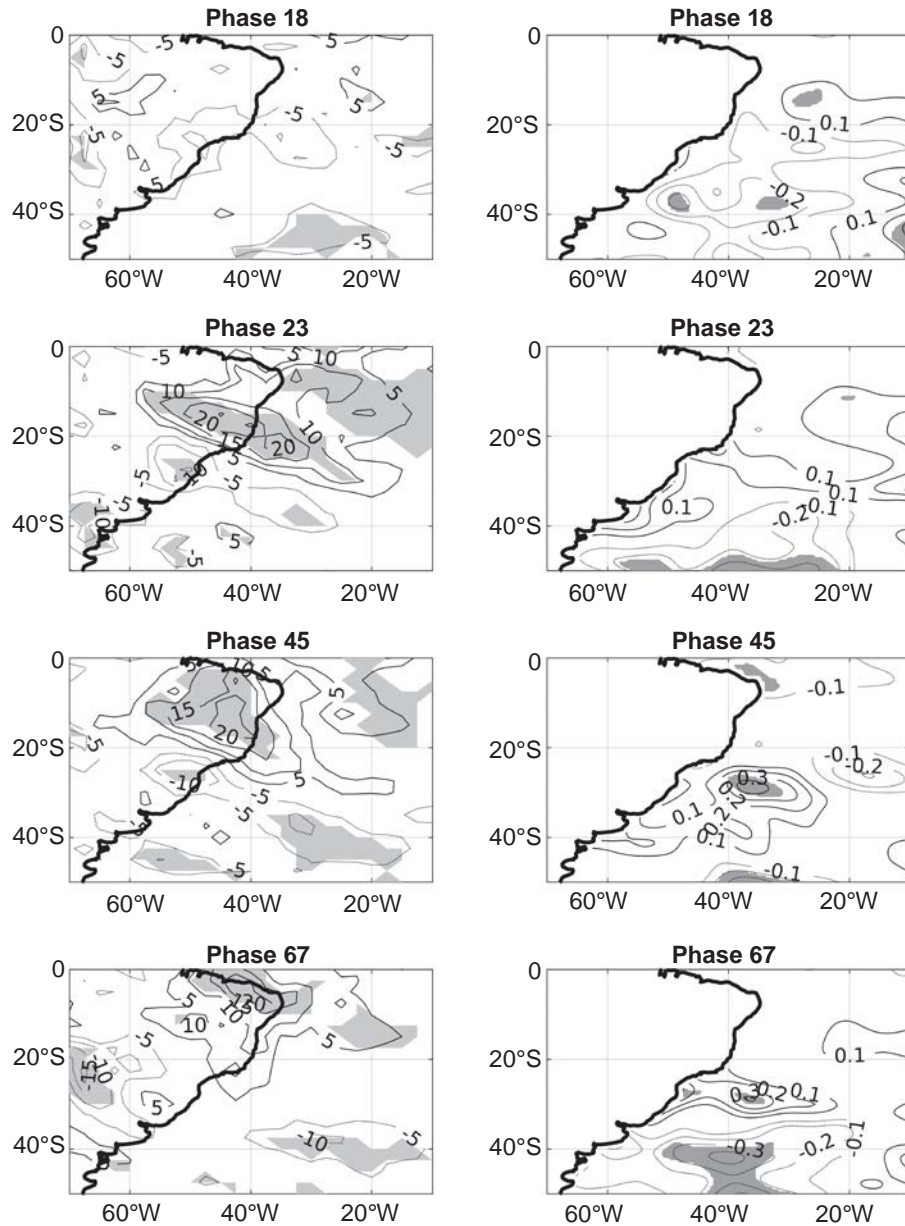


FIGURE 5 Composite of NOAA OLR anomalies (W/m^2) during different phases of the MJO (left panels). Corresponding composite of SST anomalies (K, right panels). Shading denotes regions statistically significant at 10% level

anomaly below is exactly the same leading mode of coupled variability found by Tirabassi et al. (2014), where they show that the ocean can modify the evolution of rainfall anomalies by increasing the persistence through changes in air–sea heat fluxes. Other studies have also shown that on seasonal time-scales the SACZ shifts towards the warm lobe of an SST dipole in AGCM experiments (e.g., Barreiro et al., 2002). This suggests that the SST anomaly found in phase 45 may be playing a role in inducing the observed strong response in the SACZ.

To look further into this matter we use the experiments with the regional climate model. Since observations do not show a significant response in phase 18 from now on we focus the analysis in phases 23, 45 and 67 to understand the role of air–sea coupling in MJO’s impact on eastern South

America rainfall. As shown in Figure 6 both experiments represent the southwards shift of the SACZ seen in observations with maximum anomalies in phase 45. Moreover, the location of the continental as well as the oceanic anomalies are close to the observed ones (cf., Figure 5). However, rainfall changes are stronger with larger areas of statistically significant values in the SST-forced RegCM compared to those of the RegCM-ES. In particular, the coastal and oceanic extension of the SACZ shows more coherent changes in RegCM. Also, RegCM-ES shows no rainfall anomalies over northeast Brazil, which are present in the RegCM experiment and observations, and may be consequence of the dry bias of RegCM-ES in that region (see Figure 1a). Interestingly, the composite of SST anomalies for RegCM-ES shows no significant positive SST anomalies in the

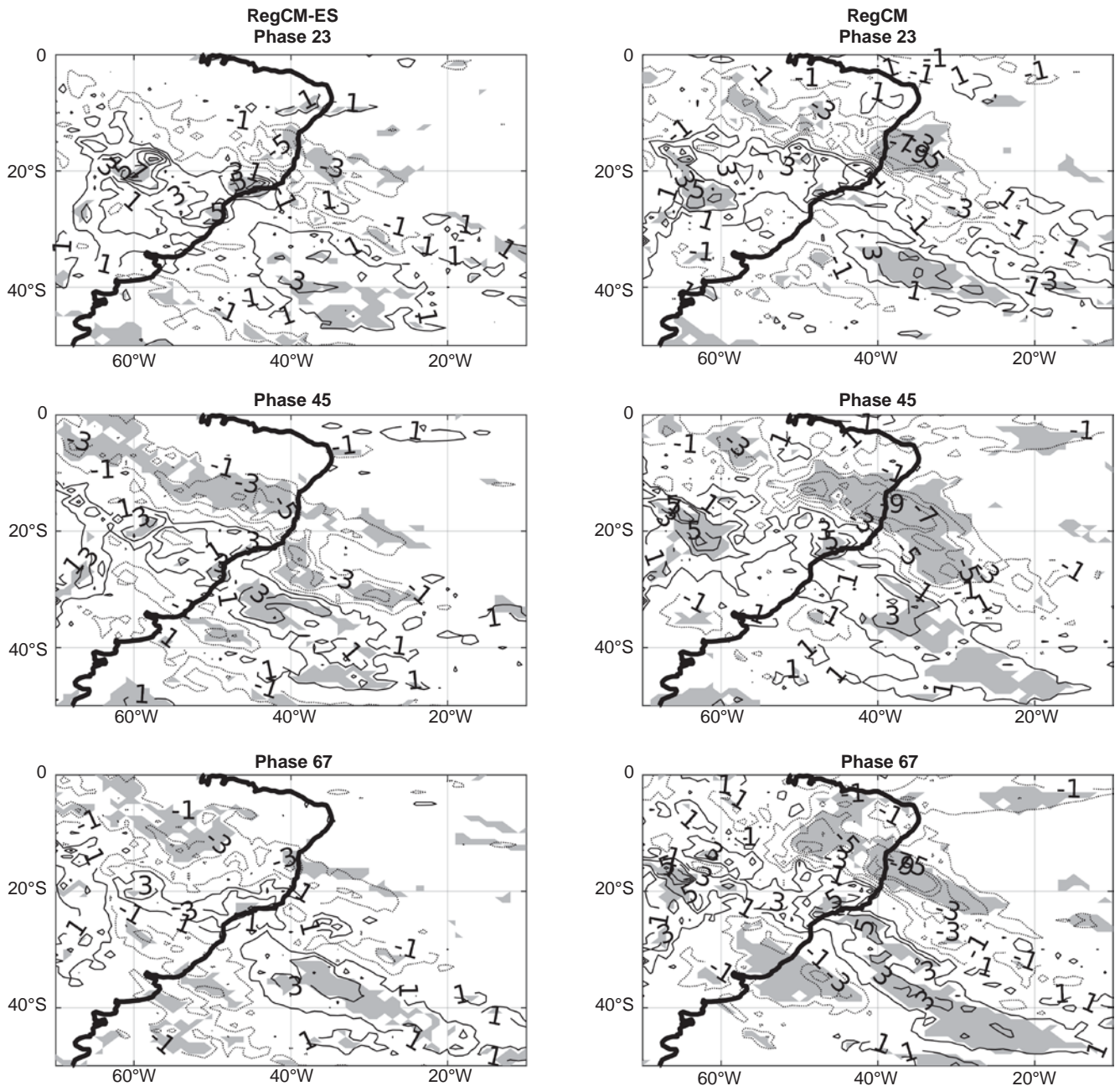
subtropical South Atlantic, contrary to observations (Figure 7). In RegCM, on the other hand, the atmosphere feels the observed SST anomalies shown in Figure 5.

3.2 | Upper- and lower-level winds response

As mentioned in the introduction MJO affects South American precipitation through tropical and extratropical teleconnections. In order to represent these teleconnections we plot the meridional wind at 300 hPa for the different phases.

Figure 8 shows the composites for ERA-Interim, RegCM and RegCM-ES. The reanalysis presents significant wind anomalies in the extratropical and tropical regions in phases 23, 45 and 67. The extratropical teleconnection, strongest in

phases 23 and 67, consists of a cyclonic anomaly with northwards flow in the southern portion of South America and southwards anomalies in the Atlantic Ocean, in agreement with Alvarez et al. (2016) and Shimizu and Ambrizzi (2015). As pointed out in Alvarez et al. (2016), this cyclonic circulation promotes anomalous upwards motion in subtropical South America. These circulation anomalies are very well reproduced in RegCM and RegCM-ES both in location and intensity, a result somehow expected as the atmospheric model is forced with the same lateral boundary conditions. The reanalysis also shows an anticyclonic anomaly in upper levels located to the east of Brazil that may induce subsidence in the SACZ during phases 23, 45 and 67 that is not present in the simulations.



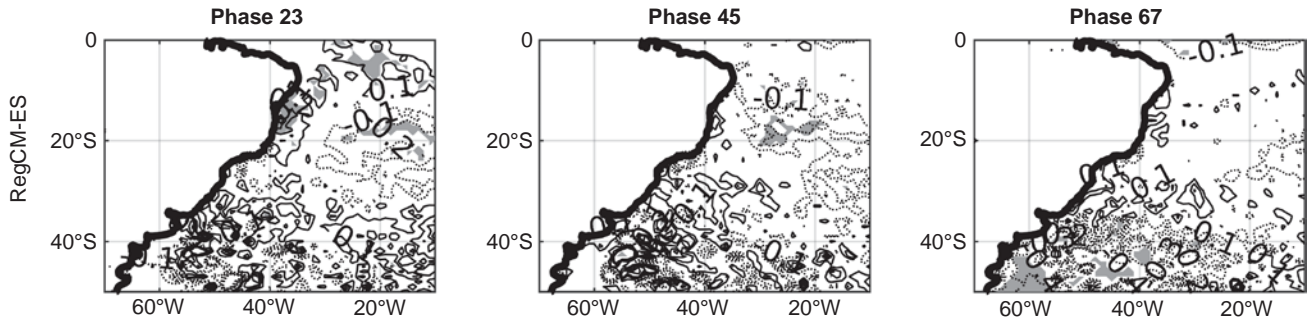


FIGURE 7 Composite of SST anomalies (K) for RegCM-ES during the different phases of the MJO. Shading as in Figure 5

We next construct the composite of surface winds for the different phases of the MJO (see Figure 9) and note that the spatial structure is similar with largest values in phase 45. In agreement with the OLR anomalies, the reanalysis shows strong surface wind convergence in the region of enhanced rainfall of the SACZ, which forms due to the existence of extratropical southerly winds and an anticyclonic circulation centred at (25°S, 35°W). During phase 45 the strongest winds are located above the SST anomaly inducing divergence to the north and convergence to the south

(Figure 10a). The anticyclonic circulation also induces divergence over northeast Brazil decreasing rainfall there. The southerlies, on the other hand, are the surface manifestation of the barotropic extratropical response seen in upper levels.

Both models are able to simulate the surface subtropical circulation anomalies seen in the reanalysis, although with different strengths (Figure 9). RegCM-ES simulates the subtropical wind convergence over the ocean as consequence of anomalous southerlies and the existence of a weak anticyclonic circulation off Brazil mainly during phases 23 and 45.

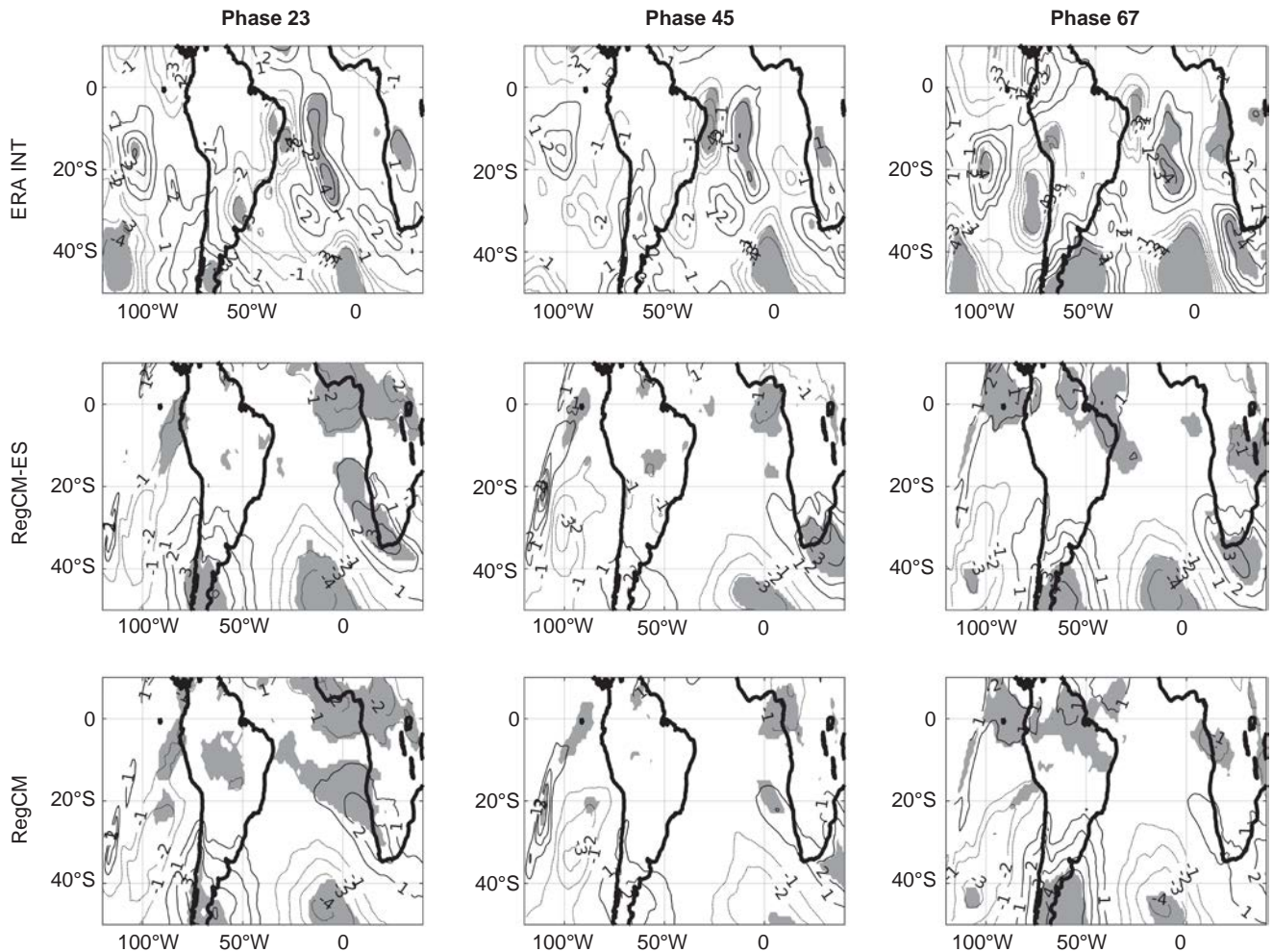


FIGURE 8 Composite of 300-hPa meridional wind anomalies (m/s) for ERA-Interim (upper panels), RegCM-ES (middle panels) and RegCM (lower panels) during the different phases of the MJO. Shading as in Figure 5

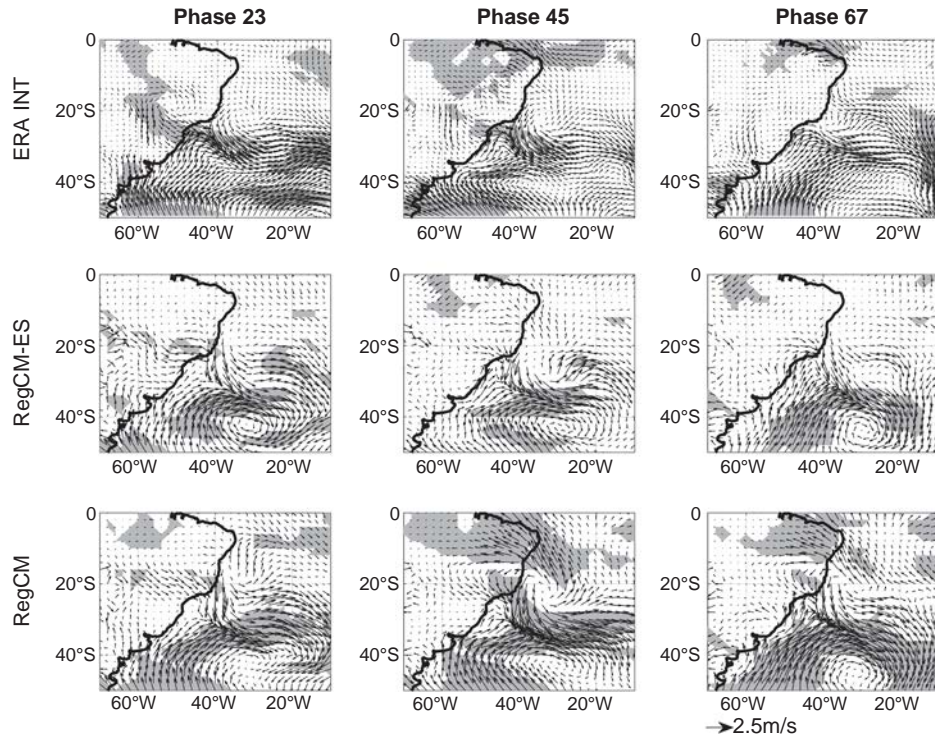


FIGURE 9 Same as Figure 8, but for surface wind anomalies (m/s)

RegCM shows a similar pattern but with stronger and more significant anomalies, in agreement with stronger rainfall anomalies. Moreover, RegCM also shows increased southern trades off northeast Brazil as also seen in the reanalysis, a feature not present in RegCM-ES. Note that in RegCM-ES the maximum wind anomalies are similar in strength as in the reanalysis but are located further south of the observed warm SST anomaly. On the other hand, in RegCM the wind intensity is larger than in observations, but the maximum is located almost on top of the SST anomaly (compare panels in Figure 10). The implied anomalous wind divergence/convergence pattern is consistent with the different rainfall anomalies seen in the simulations, where changes in the oceanic extension of the SACZ in RegCM are located further north to those in RegCM-ES (Figure 6).

4 | DISCUSSION

The RegCM and RegCM-ES are forced with the same lateral boundary conditions that drive the atmospheric model. As result, in upper levels both models show the same pattern of atmospheric circulation anomalies associated with the MJO (Figure 8), characterized by an extratropical cyclonic circulation. However, the precipitation response, though similar to observations in both models, it is larger in RegCM compared to RegCM-ES. In particular, the rainfall decrease in the northern sector of the SACZ during phases 23, 45 and 67 is much stronger in RegCM and closer to observed. Given the model setup, this differential rainfall response has to be related to air–sea coupling.

Recently, Tirabassi et al. (2014) showed that the main mode of variability in the SACZ consists of a rainfall dipole accompanied by a local SST anomaly, such that when the SACZ weakens and moves southwards a warm SST develops below. Furthermore, they show that this SST anomaly is forced through surface heat fluxes (mainly solar and latent) caused by atmospheric circulation anomalies associated with a wave train that comes from the Pacific, and that under certain conditions these SST anomalies can feed back to the atmosphere modifying rainfall anomalies in the SACZ. Here we argue for a similar behaviour: the atmospheric response in the SACZ region to the MJO teleconnection is locally modified by regional air–sea coupling.

Comparing RegCM and RegCM-ES, it is found that the stronger rainfall response in the former is related to the development of a stronger surface anticyclonic circulation off east Brazil that increases divergence (convergence) to the north (south) of the SACZ. This anticyclone is present in RegCM-ES only during phase 45 and not as well defined as in observations. On the contrary, RegCM presents a well defined anticyclonic circulation during phases 23 and 45, as seen in the reanalysis. Taking into account the results of Tirabassi et al. (2014) the key is that in RegCM-ES the model does not simulate a local SST warming that can in turn force the atmosphere. On the contrary, as the RegCM is forced with observed SST, this simulation shows the response of the surface atmosphere to the correct SST pattern forced by the MJO. In fact, the response is too strong because the anticyclonic circulation persists up to phase 67, which is not seen in observations. Thus, comparison of the results with

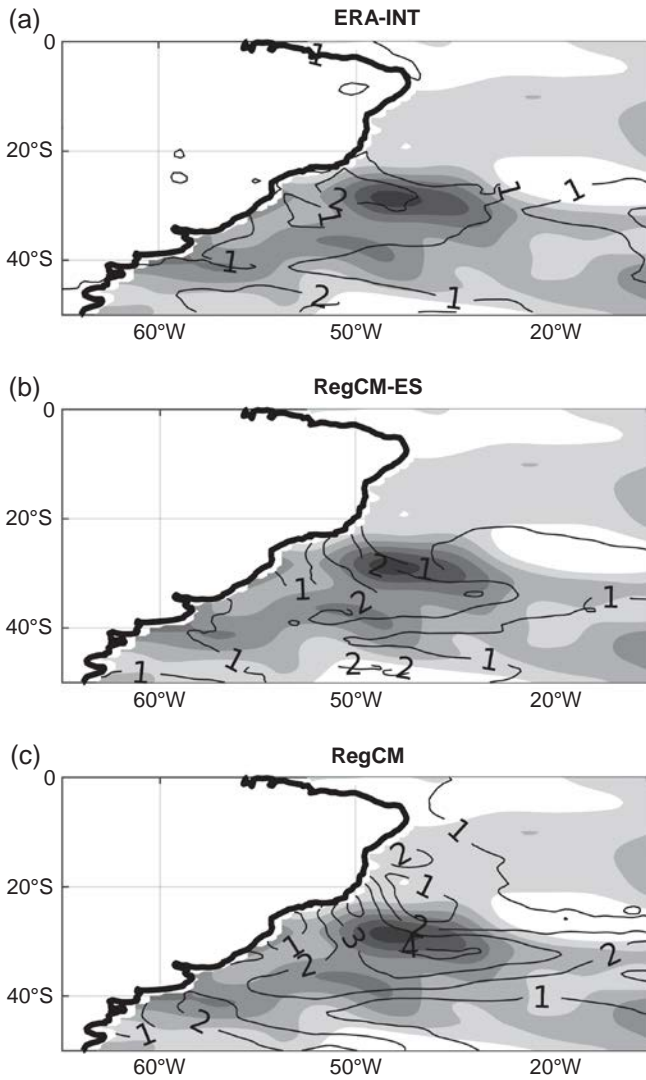


FIGURE 10 Composite of wind speed anomaly (m/s) in contours for (a) ERA-Interim, (b) RegCM-ES and (c) RegCM during phase 45 of the MJO. Shading shows ERA-Interim SST anomalies during phase 45 in the three panels. Note that this is the SST anomaly present in RegCM run, but not in RegCM-ES where it is shown for comparison purposes

RegCM and RegCM-ES supports the idea that warm the SST anomalies that are forced by the atmospheric circulation anomalies induced by the MJO in turn force the atmosphere to strengthen the MJO signal in the SACZ region. Following Chelton and Xie (2010) we hypothesize that winds over the warm SST anomaly strengthen due to increased downwards flux of horizontal momentum resulting from a more unstable atmospheric boundary layer. Sitz et al. (2017) have shown that this mechanism operates in the model. These increased surface winds in turn create a stronger divergence to the north and a stronger convergence to the south, thus maintaining the southwards shift of the SACZ. In addition the stronger winds induce more evaporation, providing a moisture source for rainfall anomalies.

As the ocean responds with a lag to the atmospheric forcing, SST anomalies seen in phase 45 should be a consequence of dynamical or thermodynamical forcing during

phase 23. Following Tirabassi et al. (2014) (and also Barreiro et al., 2004) we focus on surface heat fluxes and construct the composite of the net surface heat flux obtained from the reanalysis during the MJO (Figure 11). This composite shows that in phase 23 there is indeed a positive downwards heat flux anomaly to the south of 20°S between 20°W and 40°W. Separating into individual components of the surface heat flux shows that the net shortwave radiation is the main contributor to this positive anomaly together with a secondary contribution from the latent heat flux (lower panels Figure 11) and thus are the major forcings of the positive subtropical SST anomaly seen in phase 45. The positive shortwave anomaly during phase 23 is probably due to the weakening of the oceanic extension of the SACZ (see Figure 5). Figure 11 also shows that during phase 45 the decreased convection over the SACZ generates a strong positive net surface heat flux that maintains the warm subtropical SST anomaly up to phase 67. Interestingly, the coastal warming in the south Brazil bight observed in phase 67 seems to be consequence of strong positive latent heat fluxes associated to surface wind anomalies.

So, why does the RegCM-ES not induce these SST anomalies? According to the previous paragraph for the subtropical SST anomaly to develop in phase 45 it is important that in phase 23 there is already a weakening of the oceanic extension of the SACZ. Even though RegCM-ES has a tendency for a decreased SACZ during phase 23, convection anomalies are not strong enough and changes in the net surface heat flux are small. Thus, the warm SST does not develop. Moreover, the model has a cold bias in the subtropical region (see Sitz et al., 2017) that may play a role. Summertime is the season with strongest SST variability in the subtropical Atlantic because the ocean stratifies and the mixed layer becomes shallow. Moreover, on the sub-seasonal timescales considered here the ocean has to respond very fast and that is only possible if the mixed layer is shallow. In the coupled model, the cold bias does not allow the ocean to stratify properly during summer thus maintaining a deep mixed layer and the SST can not respond sufficiently. From Figure 7 it is possible to see that only the very strong wind anomalies during phase 45 can induce small negative SST anomalies south of 40°S in the following phase 67, as in observations.

As mentioned before, in the tropical continents rainfall and surface air temperature are negatively correlated and both experiments show this relationship, even though with different strength. Therefore, we expect that during phases 23 and 45 there should be anomalous warming in eastern Brazil. This is in fact what the reanalysis and models show (Figure 12). However, temperature anomalies in RegCM-ES are larger and have a spatial structure more similar to those in the reanalysis where the warming extends inland. In RegCM, on the other hand, the warming is limited to the coastal region. Moreover, the coastal warming observed in

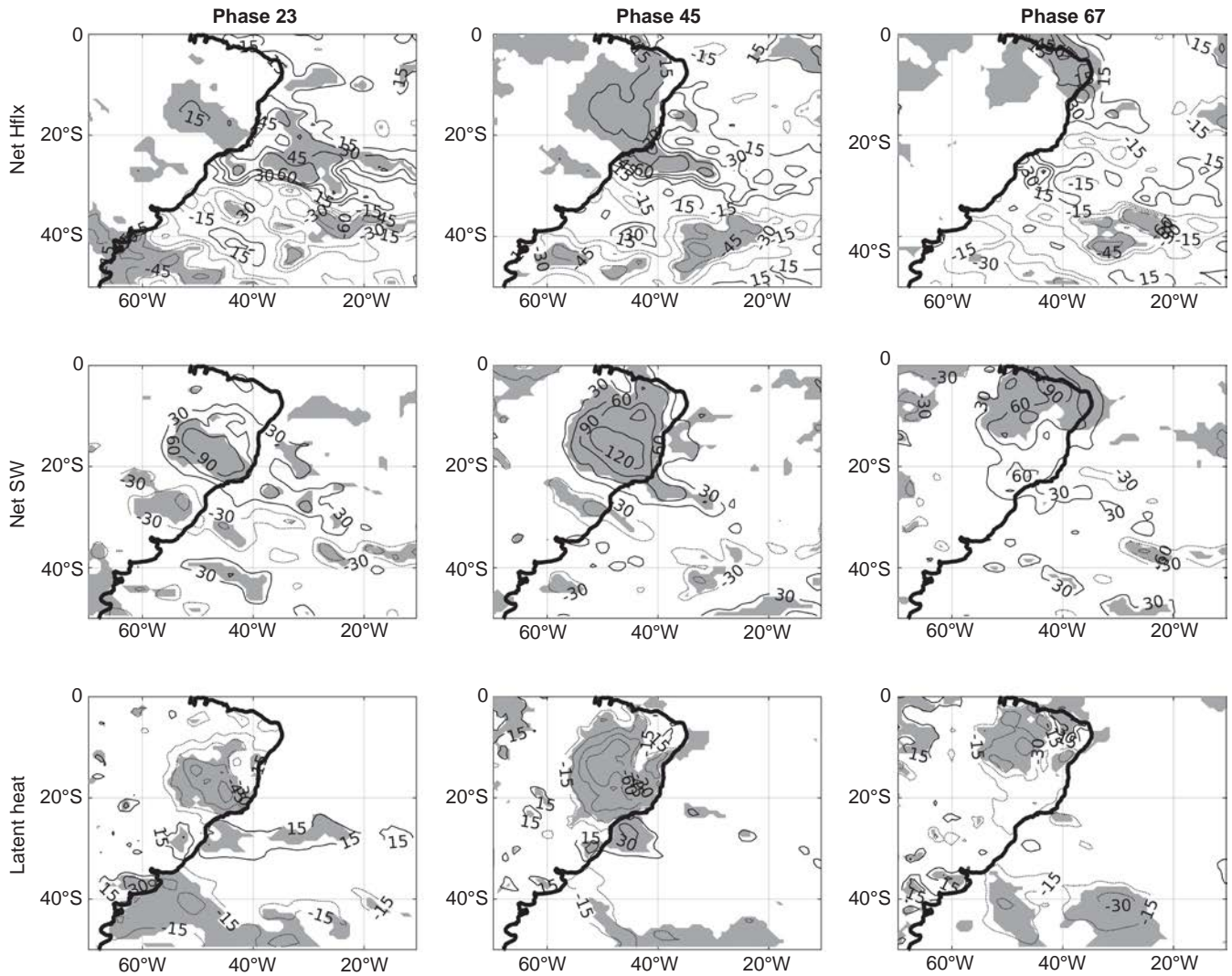


FIGURE 11 Composite of ERA-Interim net surface heat fluxes (upper panels), net downwards surface short wave radiation (middle panels) and latent heat flux (lower panels) during the different phases of the MJO. Shading as in Figure 5

phases 23 and 45 below a region of increased rainfall can be associated with increased northwesterlies. These results are consistent with the characteristics of the spatial structure of the leading mode of variability in models and observations discussed in section 2 (Figures 2–4). Note that the warming extends over the ocean during phase 45 in reanalysis and RegCM due to the local SST forcing. In RegCM-ES there is a small warming over the ocean probably related to advection of heat due to increased northerlies.

5 | SUMMARY

We have studied the role of Atlantic air–sea interaction in the remote influence of the MJO on South American climate. To do so we use reanalysis data and simulations from a regional climate model to disentangle the different processes involved. Coupled and stand-alone atmospheric model experiments are able to represent the observed influences of the MJO. In particular, models are able to represent

adequately the extratropical teleconnection associated with the MJO during phases 23, 45 and 67, which involves the development of a barotropic cyclonic anomaly over South America between 30°S and 60°S, favouring a southwards shift of the SACZ and a warming in eastern Brazil. Moreover, our results support the hypothesis that air–sea interaction is important to set up the strength of the rainfall response in the SACZ. That is, the development of a local warm SST anomaly forced by heat flux anomalies in turn feeds back into the atmosphere generating a stronger surface convergence shifting the SACZ southwards. In the absence of this SST-forced response the SACZ still shifts southwards, but anomalies are much weaker and less extensive, as simulated in RegCM-ES. It is hypothesized that alleviating the RegCM-ES cold bias in the subtropical Atlantic will result in a stronger feedback and a larger atmospheric response, eventually generating the SACZ and precipitation anomalies found in observations. Our results suggest that winds over the warm SST anomaly strengthen due to an increase in the downwards flux of momentum resulting from

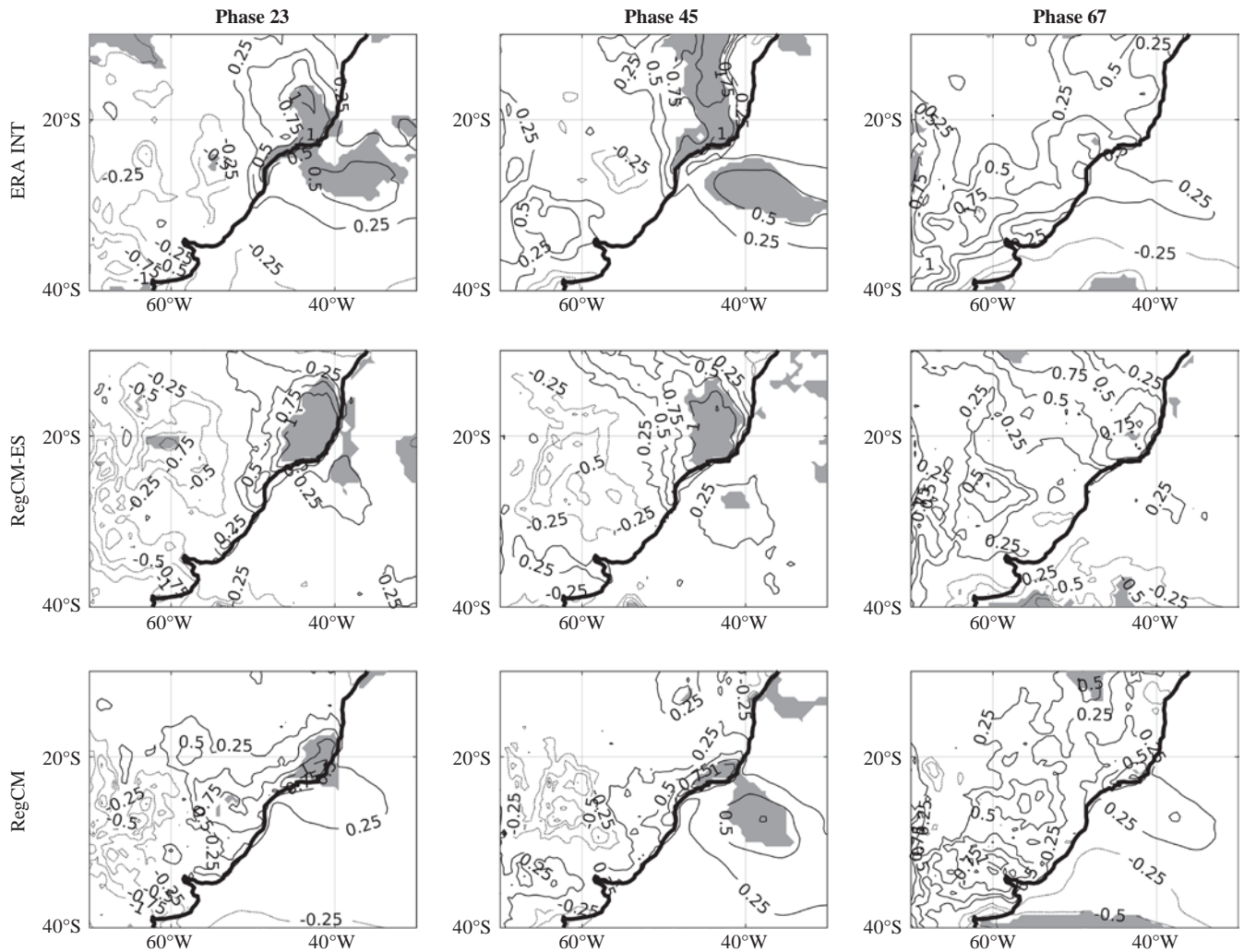


FIGURE 12 Same as Figure 8, but for surface air temperature anomalies (K)

a less stable atmospheric boundary layer (Chelton and Xie, 2010) resulting in increased divergence (convergence) to the north (south) of the SST anomaly thus maintaining the SACZ shift. This is in agreement with the role of air–sea interaction in the SACZ region proposed by Tirabassi et al. (2014). To finalize, it is worth stressing that the surface air temperature anomalies over the continent are better represented in the coupled rather than in the stand-alone model experiment, suggesting that there is a need for the consideration of air–sea coupling in order to represent adequately the remotely forced MJO signal over South America also for temperature. Overall, results suggest that as in synoptic and seasonal timescales, there is a two-way ocean–atmosphere coupling on sub-seasonal timescales in the SACZ region as well and thus prediction in this region should be performed with coupled models and not in a two-tiered framework.

ACKNOWLEDGEMENTS

Most of this study was performed during a stay of M. Barreiro at the Abdus Salam International Centre for Theoretical Physics under a Simons Associateship.

ORCID

Marcelo Barreiro  <http://orcid.org/0000-0002-7819-1607>

Ramon Fuentes Franco  <http://orcid.org/0000-0002-3085-0175>

REFERENCES

- Alvarez, M., Vera, C.S., Kiladis, G.N. and Liebmann, B. (2016) Influence of the Madden–Julian Oscillation on precipitation and surface air temperature in South America. *Climate Dynamics*, 46(1–2), 245–262. <https://doi.org/10.1007/s00382-015-2581-6>.
- Barreiro, M. and Diaz, N. (2011) Land–atmosphere coupling in El Niño influence over South America. *Atmospheric Science Letters*, 12, 351–355. <https://doi.org/10.1002/asl.348>.
- Barreiro, M., Chang, P. and Saravanan, R. (2002) Variability of the South Atlantic Convergence Zone as simulated by an atmospheric general circulation model. *Journal of Climate*, 15, 745–763.
- Barreiro, M., Giannini, A., Chang, P. and Saravanan, R. (2004) On the role of the South Atlantic atmospheric circulation in tropical Atlantic variability. In: Wang, C., Xie, S.-P. and Carton, J.A. (Eds.) *Earth’s Climate: The Ocean–Atmosphere Interaction*. Geophysical Monograph Series, Vol. 147. Washington DC: AGU, pp. 143–156.
- Barreiro, M., Chang, P. and Saravanan, R. (2005) Simulated precipitation response to SST forcing and potential predictability in the region of the South Atlantic Convergence Zone. *Climate Dynamics*, 24, 105–114. <https://doi.org/10.1007/s00382-004-0487-9>.

- Carvalho, L.M.V., Jones, C. and Liebmann, B. (2004) The South Atlantic Convergence Zone: intensity, form, persistence, relationships with intraseasonal to interannual activity and extreme rainfall. *Journal of Climate*, 17, 88–108.
- Chaves, R.R. and Nobre, P. (2004) Interactions between sea surface temperature over the South Atlantic Ocean and the South Atlantic Convergence Zone. *Geophysical Research Letters*, 31, L03204. <https://doi.org/10.1029/2003GL018647>.
- Chelton, D.B. and Xie, S.-P. (2010) Coupled ocean–atmosphere interaction at oceanic mesoscales. *Oceanography*, 23, 52–69.
- Cunningham, C.C. and Cavalcanti, I.F.A. (2006) Intraseasonal modes of variability affecting the South Atlantic Convergence Zone. *International Journal of Climatology*, 26, 1165–1180. <https://doi.org/10.1002/joc.1309>.
- Dee, D.P., Uppala, S.M., Simmons, A.J., Berrisford, P., Poli, P., Kobayashi, S., Andrae, U., Balmaseda, M.A., Balsamo, G., Bauer, P., Bechtold, P., Beljaars, A.C.M., van de Berg, L., Bidlot, J., Bormann, N., Delsol, C., Dragani, R., Fuentes, M., Geer, A.J., Haimberger, L., Healy, S.B., Hersbach, H., Hólm, E.V., Isaksen, I., Kållberg, P., Köhler, M., Matricardi, M., McNally, A.P., Monge-Sanz, B.M., Morcrette, J.-J., Park, B.-K., Peubey, C., de Rosnay, P., Tavolato, C., Thépaut, J.-N. and Vitart, F. (2011) The ERA-Interim reanalysis: configuration and performance of the data assimilation system. *Quarterly Journal of the Royal Meteorological Society*, 137, 553–597. <https://doi.org/10.1002/qj.828>.
- Donald, A., Meinke, H., Power, B., Maia, A.H.N., Wheeler, M.C., While, N., Stone, R.C. and Ribbe, J. (2006) Near-global impact of the Madden–Julian Oscillation on rainfall. *Geophysical Research Letters*, 33(9), L09704. <https://doi.org/10.1029/2005GL025155>.
- Giorgi, F., Coppola, E., Solmon, F., Mariotti, L., Sylla, M.B., Bi, X., Elguindi, N., Diro, G.T., Nair, V., Giuliani, G., Turuncoglu, U.U., Cozzini, S., Güttler, I., O'Brien, T.A., Tawfik, A.B., Shalaby, A., Zakey, A. S., Steiner, A.L., Stordal, F., Sloan, L.C. and Brankovic, C. (2012) RegCM4: model description and preliminary tests over multiple CORDEX domains. *Climate Research*, 52, 7–29.
- Gonzalez, P. and Vera, C. (2014) Summer precipitation variability over South America on long and short intraseasonal time scales. *Climate Dynamics*, 43, 1993–2007. <https://doi.org/10.1007/s00382-013-2023-2>.
- Huffman, G., Adler, R., Morrissey, M., Bolvin, D., Curtis, S., Joyce, R., McGavock, B. and Susskind, J. (2001) Global precipitation at one-degree daily resolution from multisatellite observations. *Journal of Hydrometeorology*, 2, 36–50.
- Jones, C. and Carvalho, L. (2012) Spatial-intensity variations in extreme precipitation in the contiguous United States and the Madden–Julian Oscillation. *Journal of Climate*, 25, 4898–4913.
- Jones, C., Waliser, D.E., Lau, K.M. and Stern, W. (2004) Global occurrences of extreme precipitation and the Madden–Julian Oscillation: observations and predictability. *Journal of Climate*, 17, 4575–4589.
- Liebmann, B. and Smith, C.A. (1996) Description of a complete (interpolated) outgoing longwave radiation dataset. *Bulletin of the American Meteorological Society*, 77, 1275–1277.
- Liebmann, B., Kiladis, G.N., Marengo, J.A., Ambrizzi, T. and Glick, J.D. (1999) Submonthly convective variability over South America and the South Atlantic Convergence Zone. *Journal of Climate*, 12, 1877–1891.
- Marshall, J., Adcroft, A., Hill, C., Perelman, L. and Heisey, C. (1997) A finite-volume, incompressible Navier–Stokes model for studies of the ocean on parallel computers. *Journal of Geophysical Research*, 102(C3), 5753–5766.
- Nobre, P., De Almeida, R., Malagutti, M. and Giarolla, E. (2012) Coupled ocean–atmosphere variations over the South Atlantic Ocean. *Journal of Climate*, 25, 6349–6358.
- Nogues-Paegle, J. and Mo, K.C. (1997) Alternating wet and dry conditions over South America during summer. *Monthly Weather Review*, 125(2), 279–291.
- Oleson, K., Oleson, K.W., Lawrence, D.M., Bonan, G.B., Flanner, M.G., Kluzek, E., Lawrence, P.J., Levis, S., Swenson, S.C., Thornton, P.E., Dai, A., Decker, M., Dickinson, R., Feddema, J., Heald, C.L., Hoffman, F., Lamarque, J.-F., Mahowald, N., Niu, G.-Y., Qian, T., Randerson, J., Running, S., Sakaguchi, K., Slater, A., Stöckli, R., Wang, A., Yang, Z.-L., Zeng, X. and Zeng, X. (2010) Technical description of version 4.0 of the community land model (CLM). Boulder, CO: National Center for Atmospheric Research. Technical note: NCAR/TN-478+STR.
- Paegle, J.N., Byerle, L.A. and Mo, K.C. (2000) Intraseasonal modulation of South American summer precipitation. *Monthly Weather Review*, 128, 837–850.
- Shimizu, M.H. and Ambrizzi, T. (2015) MJO influence on ENSO effects in precipitation and temperature over South America. *Theoretical and Applied Climatology*, 124, 291–301. <https://doi.org/10.1007/s00704-015-1421-2>.
- Sitz, L., Di Sante, F., Farneti, R., Fuentes-Franco, R., Coppola, E., Mariotti, L., Reale, M., Sannino, G., Barreiro, M., Nogherotto, R., Giuliani, G., Graffino, G., Solidoro, C., Cossarini, G. and Giorgi, F. (2017) Description and evaluation of the earth system regional climate model (RegCM-ES). *Journal of Advances in Modeling Earth Systems*, 9, 1863–1886. <https://doi.org/10.1002/2017MS000933>.
- de Souza, E.B. and Ambrizzi, T. (2006) Modulation of the intraseasonal rainfall over tropical Brazil by the Madden–Julian Oscillation. *International Journal of Climatology*, 26, 1759–1776. <https://doi.org/10.1002/joc.1331>.
- Tirabassi, G., Masoller, C. and Barreiro, M. (2014) A study of the air–sea interaction in the South Atlantic Convergence Zone through granger causality. *International Journal of Climatology*, 35, 3440–3453. <https://doi.org/10.1002/joc.4218>.
- Trenberth, K.E. and Shea, D.J. (2005) Relationships between precipitation and surface temperature. *Geophysical Research Letters*, 32, L14703. <https://doi.org/10.1029/2005GL022760>.
- Vera, C., Higgins, W., Amador, J., Ambrizzi, T., Garreaud, R., Gochis, D., Gutzler, D., Lettenmaier, D., Marengo, J., Mechoso, C.R., Nogues-Paegle, J., Silva Dias, P.L. and Zhang, C. (2006) Toward a unified view of the American monsoon systems. *Journal of Climate*, 19, 4977–5000.
- Wheeler, M.C. and Hendon, H.H. (2004) An all-season real-time multivariate MJO index: development of an index for monitoring and prediction. *Monthly Weather Review*, 132, 1917–1932.
- Wilks, D. (2011) *Statistical Methods in the Atmospheric Sciences*, 3rd edition. UK: Academic Press, 704 pp.